ISSN: 2833-0064

Research Article

Journal of Biopolymers and Theoretical Studies

Study of Critical Material Parameters for Curing Deformation of Aerospace Wing Composites before Numerical Simulation

Xueyong Yang[1*], Jun Xiao[2]

[1]*Unmanned Aerial Vehicles Research Institute, Nanjing University of Aeronautics and Astronautics, Nanjing 210016, China.*

[2]*College of Material Science and Technology, Nanjing University of Aeronautics and Astronautics; Nan-jing 210016, China.*

[*]Corresponding author:
Xueyong Yang, Unmanned Aerial Vehicles Research Institute, Nanjing University of Aeronautics and Astronautics, Nanjing 210016, China.

Submitted:04 Aug 2022;**Accepted**:11 Aug 2022;**Published**:24 Aug 2022

Citation: *Xueyong Yang, Jun Xiao (2022) Study of Critical Material Parameters for Curing Deformation of Aerospace Wing Composites before Numerical Simulation. J Biop Theo Stud 2(1): 60-70.*

Abstract

Because of the advantages of lightweight and high-strength integrated molding of composite materials at low cost, thus, large-scale carbon fiber composite structures are widely used in aerospace applications. However, the curing deformation of large-scale composite structures will produce a certain shape deviation, which cannot meet the needs of the installation. If forced assembly will form large installation stress, which will seriously jeopardize the mechanical properties and lifetime of the composite parts. Therefore, it is being studied to control the curing deformation of large-scale composite structures, which is important to ensure the quality of the structure, reduce the cost and improve the service life of the structure. The traditional composite parts development model requires large-scale sample testing, uncontrollable manufacturing quality, low efficiency, and other problems. In particular, the curing and molding process involves the intersection of several disciplines such as thermal, chemical and mechanics, so it is increasingly important to study the curing deformation of large-scale composite structures to improve R&D efficiency, control quality, and reduce cost.

Keywords: Fiber-Reinforced Polymer-Matrix Composites, Processed Deformation, Thermoset Composite Materials, Process Simulation, Dimensional Control, Aerospace Structures

Introduction

Due to the deformation of the wing of a certain type of UAV in the curing and molding species, the bulk deformation exceeds the assembly tolerance, and there are serious hidden dangers endangering flight safety if it is assembled on the aircraft by strong stress. Before there is no deformation prediction method, it can only rely on expensive experimental verification, resulting in a long development cycle to meet the delivery time of the equipment. In the U.S., NASA also attaches great importance to numerical analysis and prediction of composite manufacturing processes, for which the U.S. government in 2017 on NASA's Advanced Composites Research Program (AC), specifically enumerated the numerical analysis and prediction of composite manufacturing processes project for research [1,2]. The American Association of Veterinary Parasitologists (AAVP) is also proposing research programs for UAVs and applying composite manufacturing prediction techniques to the X-35. The prediction of curing deformation is the difficulty of curing deformation-molding technology, and is the main research direction of thermosetting resin-based composite materials.

The monolithic molding process for large composite components reduces the weight of the structure and the number of parts, thus reducing costs and assembly expenses. The characteristics of monolithically formed composites can cause interactions between the parts and the mold. The shrinkage of the material and the anisotropy of the material itself can lead to recoil deformation and deformation after release from the mold. This phenomenon is particularly evident in composite parts used in civil aviation and unmanned aerial vehicles, both of which produce certain dimensional deviations during the manufacturing process, making large composite components unsuitable for the stress-free installation conditions of modern aircraft.

Currently, the deformation of composite components is often studied. Parameters are optimized to reduce deformation. However, it is difficult to accurately determine the actual deformation of composite components without conducting experiments. Current scientific studies have confirmed that the variations in curing molding

can include mechanical deformation, chemical shrinkage deformation and deformation due to mold action. The prediction of curing deformation is a difficult aspect of curing deformation-molding technology and is the main research direction for thermoset resin-based composite materials.

Curing Deformation is Influenced by the Following Factors

Unstable or poor molding processes directly affect the resin content of the material components, which in turn affects the mechanical properties, expansion coefficient and curing shrinkage. Different curing process profiles directly affect the deformation of the cured molding through process parameters such as temperature and molding pressure. Since the molding stage contains a warming and holding and cooling process, the thermal expansion coefficients of the resin are different at different stages under the effect of temperature, and also after curing, the thermal expansion coefficients of the fibers, resin and mold are different, which are responsible for the curing deformation.

During the curing and molding process, there are folds and defects in the fiber lay-up, and in the composite structural parts containing corner types, which also have an effect on the rebound deformation of the composite structural parts. The prepare break and lap type can have an effect on the curing deformation of composite members. In addition, temperature gradients are generated due to different thermal conductivity. Among these are thickness gradients from the composite material, and unbalanced curing distribution, and these imbalances can lead to the generation of residual stresses and thus curing deformation.

In addition, considering the thermal force of the mold on the molded part, the surface roughness of the mold design can have an impact on the generation of frictional forces provided by the curing deformation, and the fact that the mold material and the structural material and the thermal expansion coefficient of the component do not match can have the following effects: in the case of molding with a negative mold, the deformation rebound angle of the part after demoulding is equal to the rebound angle of molding with a positive mold, and the rebound direction is just reversed; in the case of composite molds, the deformation is related to the mold structure and the design compensation method if the thermal expansion is consistent.

After the resin of the composite undergoes a transition between the viscous flow state rubber state and the glass state, the overall mechanical properties change dramatically due to a series of physical and chemical changes. The kinetic study of the numerical curing process must be carried out first. This is because the residual stresses and strains in their composites are formed during the curing process. The kinetic model of the curing reaction describes mathematically the relationship between the resin conversion rate at a given time or temperature and the resin conversion rate. Currently, domestic and foreign scientists mainly through the development of curing kinetic models describe the curing process.

Materials and Methods

The general framework technical line of research in this paper is shown in Figure 1. In addition, the superimposed coupling of cured deformation shown in Figure 2. After the resin of the composite undergoes a transition between the viscous flow state rubber state and the glass state, the overall mechanical properties change dramatically due to a series of physical and chemical changes. The kinetic study of the numerical curing process must be carried out first. This is because the residual stresses and strains in their composites are formed during the curing process. The kinetic model of the curing reaction describes mathematically the relationship between the resin conversion rate at a given time or temperature and the resin conversion rate. Currently, domestic and foreign scientists mainly through the development of curing kinetic models describe the curing process.

A non-isothermal DSC test based on the equipment model: NETZSCH DSC 200F3 was used. In this paper, a carbon fiber prepreg from Weihai Guangwei Company, grade 6508, was used, and the epoxy resin contained 40% of adhesive. The resin material used in the DSC test was physically stripped from the prepreg, and the DSC test was used to establish the curing kinetics model. Weighing samples were weighed 5~10mg using the subtractive method, and the specimens were put into the crucible as required by the experimental apparatus, as shown in Figure 3. A differential scanning calorimeter was used for the samples, and a non-isothermal test was taken, with a heating rate: 5K/min~25K/min and nitrogen gas input, flow rate: 10~20ml/min, and the apparatus was turned on to perform the experiment and record the results, as shown in Figure 4.

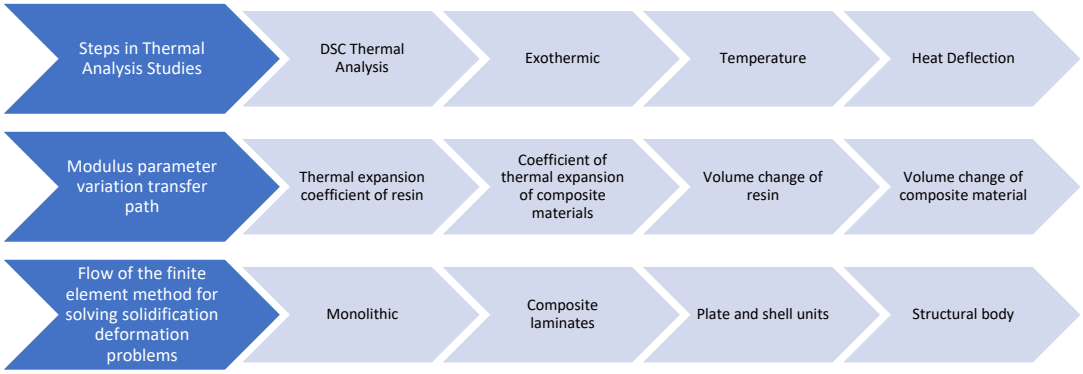

Figure 1: Research Methods and Paths of Curing Deformation

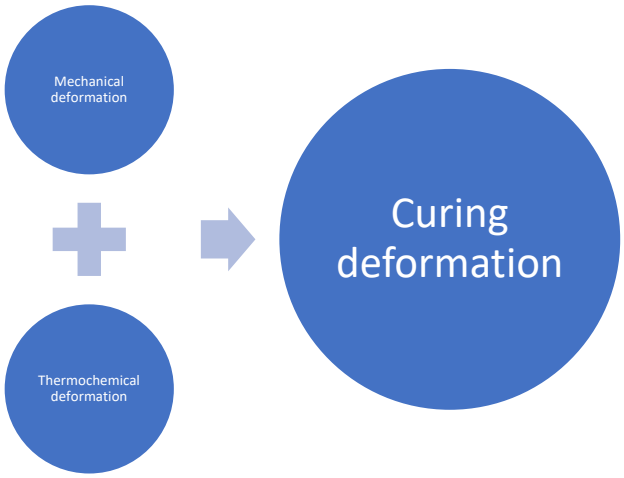

Figure 2: Superimposed Coupling of Cured Deformation

Table 1: Calculated Results of Resin Non-Isothermal DSC Test

Parameter	Value	Unit	Parameter	Value	Unit
E_{11f}	230	GPa	E_m^0	4.67E-3	GPa
$E_{22}f=E_{33}f$	17.2	GPa	E_m^0	4.67	GPa
$G_{12}f=G_{13}f$	27.6	GPa	G_m	2.33	GPa
$G_{23}f$	5.7	GPa	v_m	0.37	
$v_{12}f=v_{13}f$	0.2		ρ_m	1300	kg/m^3
$v_{23}f$	0.45				
k_{11f}	-0.9E-6	K^{-1}			
$k_{22f} = k_{33f}$	7.2E-6	K^{-1}			
ρ_f	1790	kg/m^3			

Figure 3: Sample Preparation and Differential Scanning Calorimeter Equipment

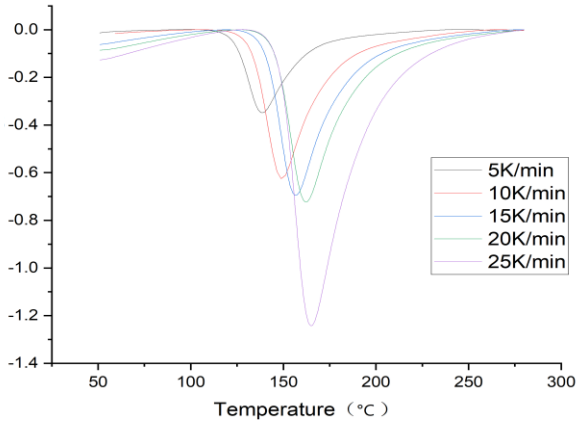

Figure 4: DSC Test Curve of Resin Curing Reaction after Unified Baseline at Different Heating Rates

Results

This section may be divided by subheadings. It should provide a concise and precise description of the experimental results, their interpretation, as well as the experimental conclusions that can be drawn. The obtained data are as follows Table 1. Calculated results of resin non-isothermal DSC test.

Table 2: Calculated Results of Resin Non-Isothermal DSC Test

Heating rate (K/min)	Peak temperature (°C)	Peak temperature (K)	Heat flow (W/g)	Enthalpy (J/g)
5 K/min	138.744	411.894	0.3306	-11.0711
10 K/min	148.843	421.993	0.56503	-21.7501
15 K/min	156.720	429.87	0.85334	-26.6368
20 K/min	162.240	435.39	1.2042	-29.4324
25 K/min	165.000	438.15	1.46988	-51.6477

The total heat of reaction of the curing reaction is obtained by averaging the above table at different rates. The activation energy of the reaction is calculated by the following equation.

$$\ln k = -\frac{E_a}{R}\frac{1}{T_p} + \ln A \qquad (1)$$

Where T_p is the peak temperature and is the heating rate.

Based on the data, a linear fit can be performed with $x = 1/T_p$ and $y = \ln k$, and the slope of

the line is obtained as follow $-\frac{E_a}{R} = -10.73467$, as shown in Figure 5.

From this, the activation energy is calculated as $E_a = R \times 10.73467 = 8.314 \times 10.73467 = 89.24805$(kJ/mol). Also obtain the intercept as lnA=23.59797, , bring in the constant R and find the coefficient $A = e^{23.59797} = 1.77202E+10$.

Table 3: Calculated Results of Resin Curing Kinetic Parameters

Parameter	E_a (kJ/mol)	A(s^{-1})
value	89.24805	1.77E+10

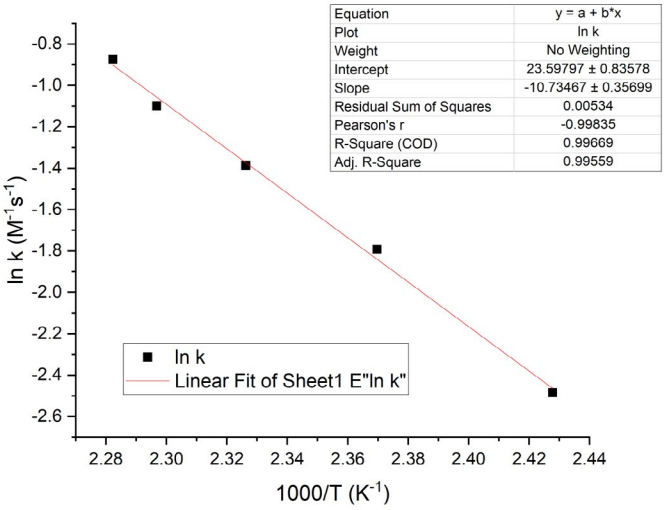

Figure 5: Fit $y = \ln K$ and $x = 1/T_p$ to the linear

After reading the DSC data and processing the data, the area, i.e., the enthalpy was obtained by integrating the transverse axes according to the relationship between the exothermic heat and time at the heating rate and obtaining the curing curve.

$$\Delta H_r = \int_{T_1}^{T_2} \frac{dH}{dt} dt \qquad (2)$$

According to the DSC exothermic-time curve as shown in Figure 6, the curing degree curves for different temperatures can be obtained by integrating the time and summarized to obtain.

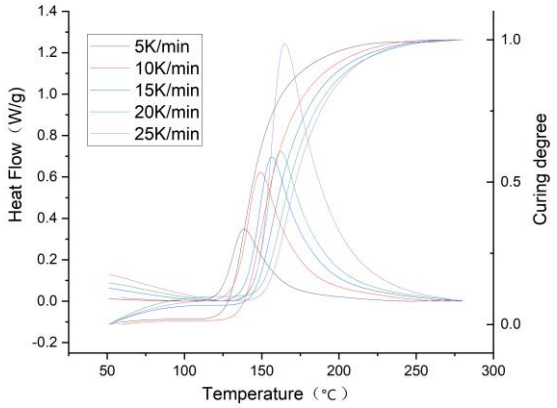

Figure 6: Curing Degree Curve and Change Curve with a Temperature Rise Rate

Reflecting the modulus change law of the curing process, for better numerical simulation, the curing degree and time in the fine structure are now expanded into a three-dimensional model, so as to reflect the modulus change law with time. Since the modulus proposed by Bogetti is linear with respect to the curing degree, the change curve of resin modulus with temperature and curing degree can be simulated according to the CHILE model, as shown in Figure 7.

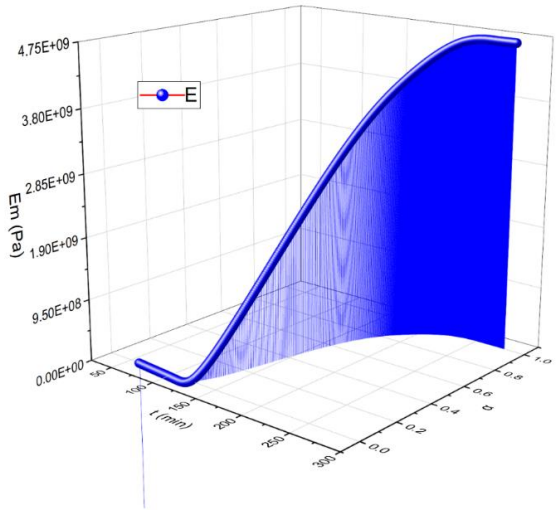

Figure 7: Linear Variation Curve of Resin Elastic Modulus with Temperature and Curing Degree

The above model indicates that the modulus of the resin is low at the initial stage of the curing degree, and when the curing degree reaches a certain value, the modulus of the resin starts to change linearly with the curing degree, and after the curing degree reaches a certain value, the modulus of the resin reaches a maximum value and does not change anymore.

The unitary model of a typical unidirectional FRP was proposed by Adli and Jansen et al, and the method proposed by Saito et al to determine the curing temperature-dependent macroscopic parameters [3-8]. The shear modulus is considered almost zero below the gel point but rises rapidly above that point due to the formation of cross-linked structures. Johnston proposed an improved model and found that the curves trend in the same direction but the relationship between resin modulus and curing degree deviates at different temperatures, suggesting that the resin modulus is not only curing degree dependent but also temperature dependent, and the following modified CHILE (Tg) model as follow [9-12].

$$E_m = \begin{cases} E_m^0 & T^* < T_{c1} \\ \dfrac{T_{c2} - T^*}{T_{c2} - T_{c1}} E_m^0 + \dfrac{T^* - T_{c1}}{T_{c2} - T_{c1}} E_m^\infty & T_{c1} \leqslant T^* < T_{c2} \\ E_m^\infty & T^* \geqslant T_{c2} \end{cases} \quad (3)$$

where $T^* = T_g - T$, T_{c1}, T_{c2} is the critical temperature at which the resin modulus starts and stops increasing, respectively, and is the temperature at which the current time is synchronized, Johnston experimentally determined the value of the above equation, E_{m}^{∞} is the resin modulus at the fully cured. α_{C1}, α_{C2} represent the boundary between the degree of development of the resin modulus in the curing assumption.

In order to make better use of the above-mentioned model and reflect the modulus change law of the curing process, and for better numerical simulation, the curing degree in the fine view structure with time is now expanded into a three-dimensional model, thus reflecting the modulus change law with time, as shown in Figure 8.

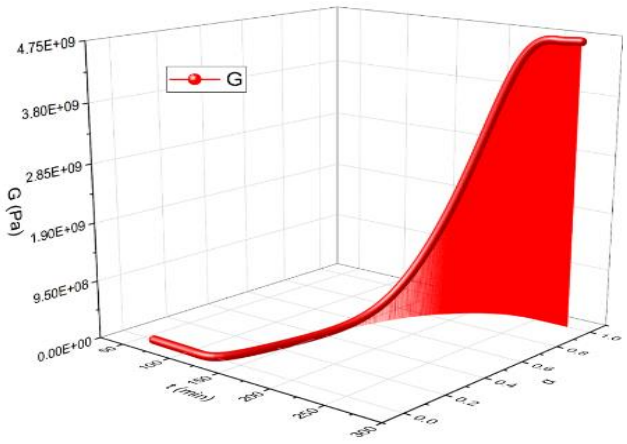

Figure 8: Non-Linear Variation Curve of Modulus Considering Temperature Field and Exotherm of Curing Reaction

After the simulated curing cycle, the contact surfaces are removed after releasing the composite component from the mold in the steady-state analysis step in order to calculate the final part deformation due to residual stresses. The boundary conditions for the mold removal phase are such that the symmetry plane of the part is allowed to slide and fix a node in the same plane in all directions. The deformation of the composite part is measured by being perpendicular to the direction of shrinkage. Temperature conversion was measured experimentally by Abouhamzeh and Bellini et al. using the temperature transformation, the effect of temperature on viscoelastic materials can be converted to a time scale and the transformation is referred to the previous generalized Maxwell model to obtain the initial stiffness matrix [13-20].

Zappino et al. made simulations where the results approximated the experimental values, so by varying the thermal expansion coefficient and thickness of the shear layer, these parameters are valid for a given curing pressure and size [21]. Residual stresses can usually be defined as the sum of the following: initial pressure, thermochemical, thermal expansion and shrinkage, with coefficients of thermal expansion and chemical shrinkage in three directions, containing uncured and cured. Since the equivalent thermal expansion coefficient cannot model the chemical shrinkage that may occur at constant temperature. Therefore, the minimum incremental step was adjusted to simulate the chemical shrinkage, the shrinkage strain of the resin was calculated by the degree of resin curing, and the curve was obtained experimentally and by fitting. In curing, the time curing temperature superposition method is used, containing thermochemical, thermal expansion and shrinkage, which are simulated in three directions, respectively.

The curing pressure definition function involves two effects, on the one hand, the resin content affects the curing degree function distribution and chemical shrinkage, and on the other hand, the pressure affects the resin content distribution in each part. Therefore, the determination of thermal curing deformation is a good way to predict the thermal and chemical shrinkage stresses based on the temperature and curing degree fields. The curing kinetics of the laminate was found to be a controlling equation mainly influenced by temperature and degree of cure:

$$\sigma_{ij}(t) = \int_{-\infty}^{t} Q_{ij,kl}(\alpha, T, t) \frac{\partial}{\partial \tau} \left[\varepsilon_{kl}(\tau) - \varepsilon_{kl}^{tc}(\tau) \right] d\tau$$

where $Q_{ij,kl}(\alpha,T,t)$ is the additional stress, $Q_{ij,kl}(\alpha,T,t)$ is the stiffness, α is the degree of cure of the resin, τ is the time, ε_{kl} is the total strain, ε_{kl}^{tc} is the chemical strain, and T is the temperature.

At the end of curing, after removal of the part from the mold and deformation due to the axial stress distribution through the thickness

$$M(x)\big|_{k\Delta t} = M(x)\big|_{(k-1)\Delta t} + \Delta M(x)\big|_{k\Delta t},$$

the deformation can be expressed by the unbalanced moment

$$\frac{d^2 v}{dx^2} = \frac{M(x)}{(EI)_{eff}},$$

where $(EI)_{eff}$ is the bending stiffness at the end of the curing cycle.

The temperature distribution in the composite during curing can be obtained using nonlinear transient heat transfer analysis (including internal heat consumption).

The steps of the numerical simulation experiment are as follows:

1) Using laser underlayment machine to underlay the CAD designed drawing.

2) Prepare 40 layers of lay-up material with thickness 0.28 mm, stacking order as shown in Table 4 and as shown in Figure 9.

3) Composite multilayer shell module with COMSOL 6.0 software, shell heat transfer module, as well as solid mechanics module and chemical reaction kinetics module, multi-physical fields were coupled for analysis.

4) To verify the experimental validation of the process, we prepared prepreg materials in different orientations, as shown in Figure 10. The experimental validation of the process were as follow: Within 45 minutes of the heating stage, the heating rate is 0.5~2K/min, reaching 85℃, holding time 30min, heating to 130℃ within half an hour, holding time 120min, then cooling 240min, cooling with the furnace, cooling rate 0.5K/min or less, then air cooling.

5) Multi-layer panel shell model and wing panel shell model were setup as shown in Figure 11.

6) Temperature distribution of heat sources were used for multi-layer panel shell and wing panel as shown in Figure 12.

7) From 0 to 0.28mm, under the total cases, Stress for multi -layer panel shell and wing panel were shown in Figure 13, Figure 14, Figure 15, Figure 16 and Figure 17.

Table 4: Orientation of carbon fiber/epoxy laminates

Layer Number	Fiber Orientation 1	Fiber Orientation 2
1-5	0	0
6-10	45	45
11-15	-45	-45
16-20	90	90
21-25	90	90
26-30	-45	45
31-35	45	-45
36-40	0	0

Figure 9: The Stacking Sequence of the Carbon/Epoxy Laminate is from Bottom to Top for each Layer of Fiber Orientation

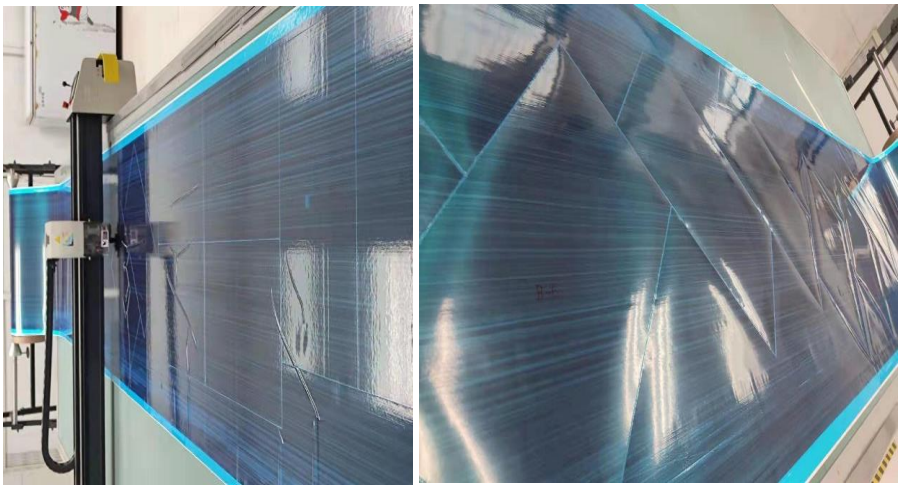

Figure 10: Cutting of Materials with Different Orientations for Undercutting

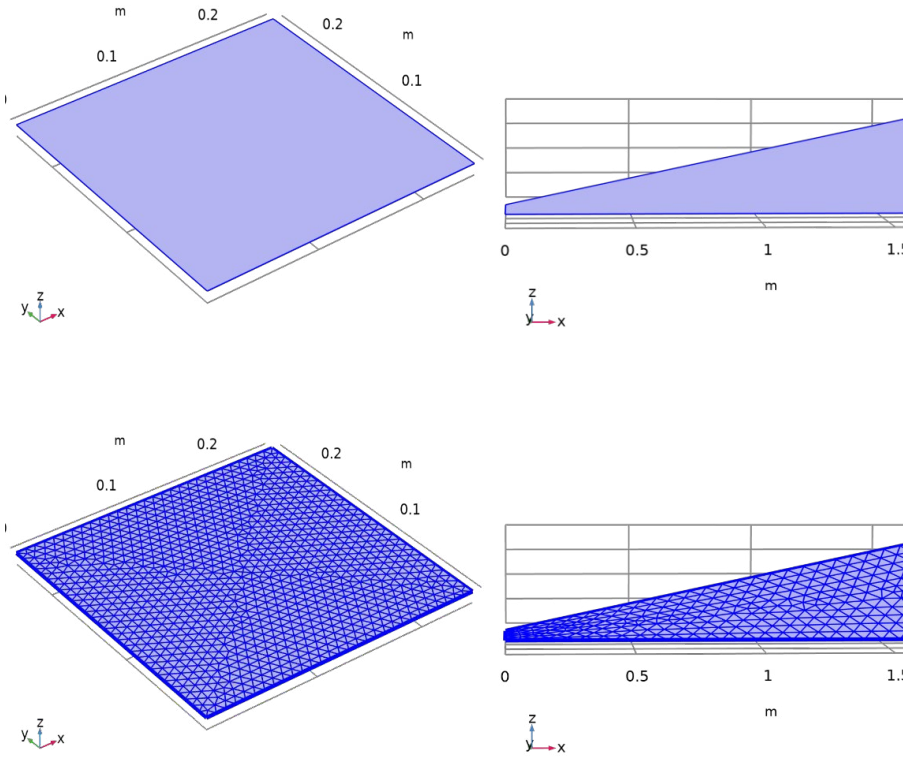

Figure 11: Multi-layer Panel Shell Model and Wing Panel Shell Model

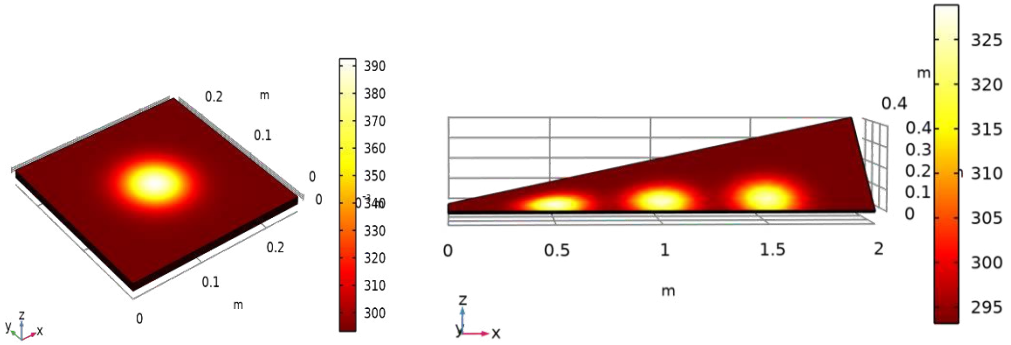

Figure 12: Temperature Distribution of Heat Sources for Multi-Layer Panel Shell and Wing Panel

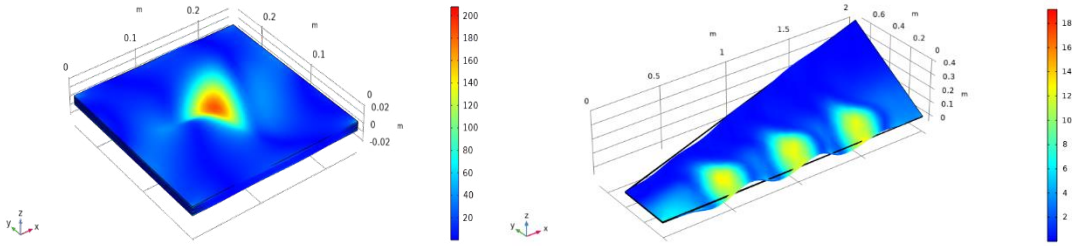

Figure 13: Von Mises Stress for Multi -Layer Panel Shell and Wing Panel (MPa)

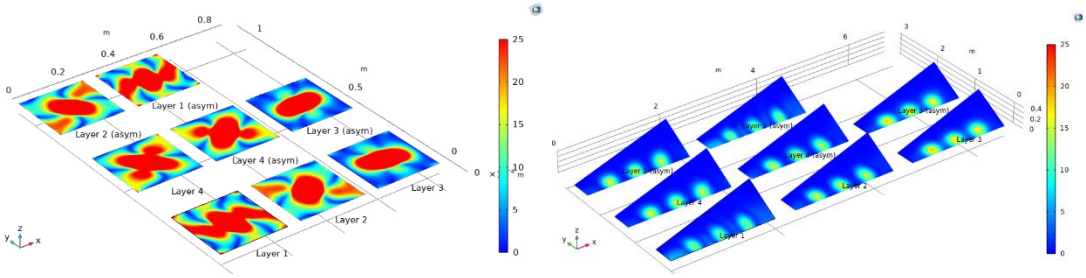

Figure 14: Type II Piola-Kirchhoff Stresses for Multi-Layer Panel Shell and Wing Panel, Laminate Coordinate System 11 Components (MPa), Thickness: 0 ~ 0.07 mm

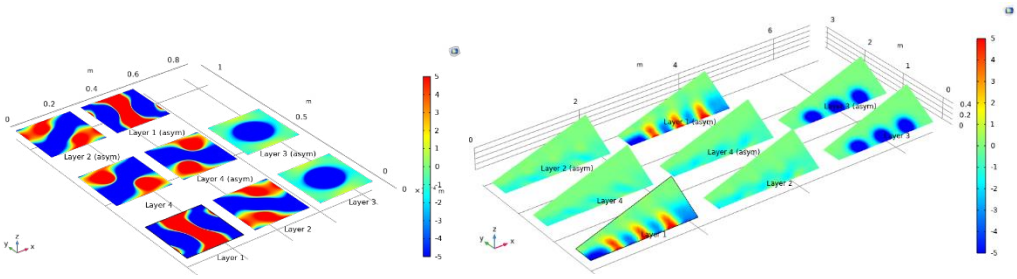

Figure 15: Type II Piola-Kirchhoff stresses for multi-layer panel shell and wing panel, laminate coordinate system 11 components (MPa), thickness: 0.07 ~ 0.14 mm

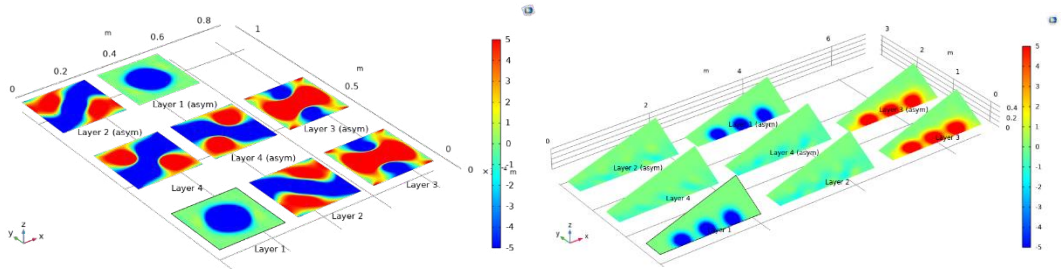

Figure 16: Type II Piola-Kirchhoff stresses for multi-layer panel shell and wing panel, laminate coordinate system 11 components (MPa), thickness: 0.14 ~ 0.21 mm

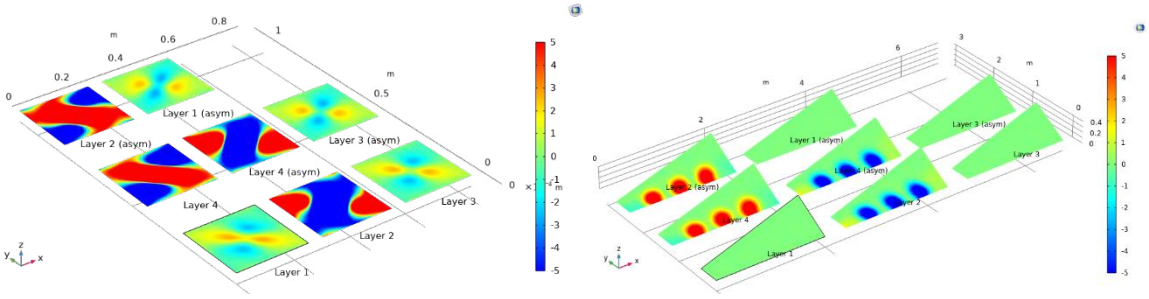

Figure 17: Type II Piola-Kirchhoff stresses for multi-layer panel shell and wing panel, laminate coordinate system 11 components (MPa), thickness: 0.21 ~ 0.28mm

Discussion

Curing Mold Suppression

Reduce the influence of mold molding specific gravity, according to this special case, according to the characteristics of the resin curing curve adopted a mold with high thermal conductivity, the general case using a mold material with a similar conductivity. The measurement process used calibrated gauges and molds.

Suppression of Molding Pressure

The quality control of the test parts was carried out during the test process. When the molding pressure was 0.080 MPa, there was a sample molding with uneven glue content; when the pressure was increased to 0.096 MPa, the bubble defects were significantly reduced and the uneven glue content was significantly improved, which reduced the degree of influence on the distortion.

Suppression of Cooling Time

As the mechanical properties of the composites change due to the rate of thermal curing reaction. It is known that the greater the rate of heating, the earlier the curing process is completed; in the cooling phase, the slower the rate of curing reaction, which is conducive to the control of curing distortion.

Inhibition of Lay-Up Design

When laying the prepreg, the polymer viscosity is low enough to ensure maximum fit to the mold and guarantee the consistency of the thermal expansion coefficient, which can be beneficial to reduce distortion.

Conclusions

Based on the simulation results, the following findings can be made toward the manufacturing process of unidirectional composite structures. Reducing the thermal contact conductivity between the composite part and the mold speeds up curing because it reduces the heat transfer when the epoxy exotherms. This results in less deformation due to the lower temperature gradient along the thickness of the composite component. This factor becomes more important as the thickness of the composite member increases. The coefficient of thermal expansion can be reduced by using a low thermal conductivity layer between the composite member and the mold, or by physically reducing the surface contact between the mold and the composite member through a new mold surface design (which requires an optimized design). Reducing the rebound deformation can only be done physically by reducing the surface contact between the mold and the composite member. It can be noted that the same parameters lead to a reduction of the rebound deformation during the thermal analysis.

The factors responsible for the generation of residual stresses and deformations during hot pressing curing can be summarized as follows: thermal strain is the result of a mismatch between the thermal properties of the laminate layers, the temperature gradient and the degree of resin curing and the coefficient of thermal expansion between the part and the mold. Curing shrinkage is due to volume reduction because of increased density. The shrinkage strain is higher in the direction transverse to the fibers than in the direction of the fibers, which will be largely constrained.

(1) The measured and predicted deformation angles closely match. However, the evaluation of corner shape variation shows deviations between predictions and measurements and represents a straightforward approach to predicting deformation in the fabrication of large-scale composite structures based on minimal experi-

mental work.

(2) The method requires only one configuration-specific parameter for the simulation in the form presented. This is appropriate as long as the laminate layup is constant throughout the part. Considering locally varying layups, it should be verified that the obtained configuration-specific parameters can be transferred between individual layups.

(3) My experimental studies have shown that the angle of deformation depends to a large extent on the laminate layup as long as the layup characteristics are significantly different. Small changes in plies due to the addition of a single ply (symmetry preservation) do not significantly affect the angle of deformation obtained. However, if the laminate changes significantly within a part.

Author Contributions: software, Xueyong Yang; formal analysis, Jun Xiao; All authors have read and agreed to the published version of the manuscript.

Funding: This work is supported by the National Natural Science Foundation of China (Grant No. 52075251).

References

1. Bi, F. Y., Yang, B., Jin, T. G., Liu, W. J., Liu, C. X., & Wang, X. H. (2020, September). Sensitivity Analysis of Influencing Factors on Mould Surface Deformation of Resin Matrix Composites by Autoclave Moulding. In 2020 4th Annual International Conference on Data Science and Business Analytics (ICDSBA) (pp. 258-261). IEEE.
2. Henning, F., Kärger, L., Dörr, D., Schirmaier, F. J., Seuffert, J., & Bernath, A. (2019). Fast processing and continuous simulation of automotive structural composite components. Composites Science and Technology, 171, 261-279.
3. Adli, A. R., & Jansen, K. M. (2016). Numerical investigation and experimental validation of residual stresses building up in microelectronics packaging. Microelectronics Reliability, 62, 26-38.
4. Hirsekorn, M., Marcin, L., & Godon, T. (2018). Multi-scale modeling of the viscoelastic behavior of 3D woven composites. Composites Part A: Applied Science and Manufacturing, 112, 539-548.
5. Abouhamzeh, M., Sinke, J., Jansen, K. M. B., & Benedictus, R. (2015). A new procedure for thermo-viscoelastic modelling of composites with general orthotropy and geometry. Composite Structures, 133, 871-877.
6. Jansen, K. M., & Öztürk, B. (2013). Warpage estimation of a multilayer package including cure shrinkage effects. IEEE Transactions on Components, Packaging and Manufacturing Technology, 3(3), 459-466.
7. Jansen, K. M. B., De Vreugd, J., & Ernst, L. J. (2012). Analytical estimate for curing-induced stress and warpage in coating layers. Journal of Applied Polymer Science, 126(5), 1623-1630.
8. Jansen, T., & Zarges, C. (2011, January). Analysis of evolutionary algorithms: From computational complexity analysis to algorithm engineering. In Proceedings of the 11th workshop proceedings on Foundations of genetic algorithms (pp. 1-14).
9. Traiforos, N., Turner, T., Runeberg, P., Fernass, D., Chronopoulos, D., Glock, F., ... & Hartung, D. (2021). A simulation framework for predicting process-induced distortions for precise manufacturing of aerospace thermoset composites. Composite Structures, 275, 114465.
10. Dai, J., Xi, S., & Li, D. (2019). Numerical analysis of curing residual stress and deformation in thermosetting composite laminates with comparison between different constitutive models. Materials, 12(4), 572.
11. Liang, Q., & FENG, X. (2019). Residual stress and structural distortion analysis for the curing process of SRM composite case. Journal of Solid Rocket Technology, 42(5), 628-634.
12. Zhang, G., Wang, J., Ni, A., Hu, H., Ding, A., & Li, S. (2019). Process-induced deformation of L-shaped variable-stiffness composite structures during cure. Composite Structures, 230, 111461.
13. Abouhamzeh, M., Sinke, J., & Benedictus, R. (2019). A large displacement orthotropic viscoelastic model for manufacturing-induced distortions in Fibre Metal Laminates. Composite Structures, 209, 1035-1041.
14. Abouhamzeh, M., Sinke, J., & Benedictus, R. (2019). Prediction models for distortions and residual stresses in thermoset polymer laminates: An overview. Journal of Manufacturing and Materials Processing, 3(4), 87.
15. Abouhamzeh, M., Sinke, J., Jansen, K. M. B., & Benedictus, R. (2015). Kinetic and thermo-viscoelastic characterisation of the epoxy adhesive in GLARE. Composite Structures, 124, 19-28.
16. Bellini, C., Di Cocco, V., Iacoviello, F., & Sorrentino, L. (2021). Numerical model development to predict the process-induced residual stresses in fibre metal laminates. Forces in Mechanics, 3, 100017.
17. Bellini, C., Polini, W., & Sorrentino. (2014). A new class of thin composite parts for small batch productions. Advanced Composites Letters, 23(5), 096369351402300502.
18. Bellini, C., & Sorrentino, L. (2018). Analysis of cure induced deformation of CFRP U-shaped laminates. Composite Structures, 197, 1-9.
19. Bellini, C., Sorrentino, L., Polini, W., & Corrado, A. (2017). Spring-in analysis of CFRP thin laminates: numerical and experimental results. Composite Structures, 173, 17-24.
20. Lange, J., Toll, S., Månson, J. A. E., & Hult, A. (1997). Residual stress build-up in thermoset films cured below their ultimate glass transition temperature. Polymer, 38(4), 809-815.
21. Zappino, E., Zobeiry, N., Petrolo, M., Vaziri, R., Carrera, E., & Poursartip, A. (2020). Analysis of process-induced deformations and residual stresses in curved composite parts considering transverse shear stress and thickness stretching. Composite Structures, 241, 112057.